Optimality Self Online Monitoring (OSOM) for Performance Evaluation and Adaptive Sensor Fusion

Chun Yang
Sigtem Technology, Inc.
San Mateo, CA 94402
chunynag@sigtem.com

Erik Blasch
Air Force Research Lab
WPAFB, OH 45433
erik.blasch@wpafb.afb.mil

Ivan Kadar
Interlink Sciences Systems, Inc.
Lake Success, NY 11042
ikadar@SystemsSciences.com

Abstract – The performance of a tracking filter can be evaluated in terms of the filter's optimality conditions. Testing for optimality is necessary because the estimation error covariance as provided by the filter is not a reliable indicator of performance, which is known to be "optimistic" (inconsistent) particularly when there are model mismatches and target maneuvers. The conventional root-mean square (RMS) error value and its variants are widely used for performance evaluation in simulation and testing but it is not feasible for real-time operations where the ground truth is hardly available. One approach for real-time reliability assessment is optimality self online monitoring (OSOM) investigated in this paper. Statistical tests for optimality conditions are formulated. Simulation examples are presented to illustrate their possible use in evaluation and adaptation.

Keywords: Tracking, Optimality, Evaluation, Adaptation.

1 Introduction

From design, procurement, to deployment, performance evaluation remains one of the issues that target tracking and automatic target recognition (ATR) system engineers, government buyers, and systems operators must address in different phases of the systems' life cycle. In design and test stages, performance evaluation is relatively easier not only because the ground truth is available, but also because the tests can be repeated. During deployment, however, the ground truth about a target can never be known *a priori* and there seldom exists a second chance in a time-critical hostile environment to verify algorithm performance.

There are at least two types of performance evaluation. One is *comparative* (and competitive) among a variety of algorithms or designs wherein a set of performance metrics are used to rank the algorithms or designs for one-out-of-many selection. It typically requires the ground truth. In most cases, no single algorithm or design would prevail for all performance metrics and no single metric can capture all performance aspects under all conditions (i.e., scenarios). The other type of performance evaluation is *absolute*, which is concerned with a particular algorithm or design in run time. The second type of performance evaluation is the focus of this paper.

Although comparative metrics can be used when the ground truth is available [4, 18], an alternative approach is to make use of design specs and optimality conditions as a means for performance evaluation. Indeed, modern target tracking and ATR system designs are model-based and they are optimized or tuned with respect to certain design criteria or cost functions. When the design conditions are met, the filter is expected to perform within specs. In a sense, each filter ought to have an *optimality self online monitoring* (OSOM) module to ascertain if the operation is optimal and if not, to provide timely feed back for online tuning and adaptation. In a sense, this forms a closed loop involving sensor management, thus related to such research areas as adaptive control and fault detection and isolation (FDI).

This paper presents an OSOM system for target tracking filters and their fusion via adaptive sensor management. It monitors the optimality conditions of a tracking filter using statistical tests (e.g., normality and whiteness) based on the innovation sequence and relates the deviation from the optimal conditions to the errors developed in the target state. It can further calculate the actual process and measurement noise covariance matrices as compared to those used by the filter. Together with the sensitivity of optimality conditions with respect to various filter parameters (e.g., Q, R, P_0), it enables on-line tuning or adaptation so as to maintain the optimality conditions.

The paper is organized as follows. In Section 2, a typical tracking filter is described together with analytic performance prediction. In Section 3, a series of optimality tests are presented for performance monitoring. In conjunction with OSOM, methods for filter tuning, adaptive distributed fusion, and active sensor management are outlined in Section 4. Section 5 concludes the paper with some future work. Simulation examples are presented to illustrate the OSOM procedure in the paper.

2 Tracking Filter & Performance

Tracking filter design strikes a balance between noise performance and dynamic responsiveness to target maneuvers. Given the sensor error characteristics, the design boils down to the choice of covariance for process noise, which is a modeling tool widely used in the Kalman filter to deal with uncertainty. However, the estimation error covariance of the Kalman filter becomes inconsistent when large maneuvers occur. The sensor noise only covariance and steady-state biases or lags in position and velocity may be used instead. Design optimization then consists of finding the filter gain given the maximum possible maneuver that minimize the overall root mean square (RMS) errors [6].

2.1 Target & Measurement Truth Models

Consider the following target model:

$$\mathbf{x}_{k+1} = \mathbf{F}_k \mathbf{x}_k + \mathbf{G}_k(\mathbf{u}_k + \mathbf{v}_k) \quad (1a)$$

$$\mathbf{z}_k = \mathbf{H}_k \mathbf{x}_k + \mathbf{w}_k \quad (1b)$$

Report Documentation Page

Form Approved
OMB No. 0704-0188

1. REPORT DATE	2. REPORT TYPE	3. DATES COVERED
JUL 2008		**00-00-2008 to 00-00-2008**

4. TITLE AND SUBTITLE	5a. CONTRACT NUMBER
Optimality Self Online Monitoring (OSOM) for Performance Evaluation and Adaptive Sensor Fusion	5b. GRANT NUMBER
	5c. PROGRAM ELEMENT NUMBER
6. AUTHOR(S)	5d. PROJECT NUMBER
	5e. TASK NUMBER
	5f. WORK UNIT NUMBER
7. PERFORMING ORGANIZATION NAME(S) AND ADDRESS(ES) **Air Force Research Laboratory,Wright Patterson AFB,OH,45433**	8. PERFORMING ORGANIZATION REPORT NUMBER
9. SPONSORING/MONITORING AGENCY NAME(S) AND ADDRESS(ES)	10. SPONSOR/MONITOR'S ACRONYM(S)
	11. SPONSOR/MONITOR'S REPORT NUMBER(S)

12. DISTRIBUTION/AVAILABILITY STATEMENT
Approved for public release; distribution unlimited

13. SUPPLEMENTARY NOTES
11th International Conference on Information Fusion, June 30 ? July 3, 2008, Cologne, Germany.

14. ABSTRACT
see report

15. SUBJECT TERMS

16. SECURITY CLASSIFICATION OF:			17. LIMITATION OF ABSTRACT	18. NUMBER OF PAGES	19a. NAME OF RESPONSIBLE PERSON
a. REPORT **unclassified**	b. ABSTRACT **unclassified**	c. THIS PAGE **unclassified**	**Same as Report (SAR)**	**8**	

where for the one-dimensional (1D) case (i.e., in one coordinate, say, the *x*-axis) the following variables and matrices are defined:

$$\mathbf{x}_k = [x_k \quad \dot{x}_k]^T \tag{2a}$$

$$\mathbf{F}_k = \begin{bmatrix} 1 & T \\ 0 & 1 \end{bmatrix} \tag{2b}$$

$$\mathbf{G}_k = \begin{bmatrix} \frac{T^2}{2} & T \end{bmatrix}^T \tag{2c}$$

$$\mathbf{H}_k = [1 \quad 0] \tag{2d}$$

T is the sampling interval, $\mathbf{u}_k$ is an unknown deterministic acceleration input, $\mathbf{v}_k$ is a random acceleration process with zero mean and variance σ_v^2, $\mathbf{z}_k$ is the measurement, and $\mathbf{w}_k$ is the measurement noise with zero mean and variance $\mathbf{R}_k = \sigma_w^2$.

2.2 Kalman Filter & α-β Filter

Given the target motion and measurement models in (1) and (2), the corresponding Kalman filter consists of the time update (propagation) step (if $\mathbf{u}_k$ is known):

$$\hat{\mathbf{x}}_{k+1|k} = \mathbf{F}_k \hat{\mathbf{x}}_{k|k} + \mathbf{G}_k \mathbf{u}_k \tag{3a}$$

$$\mathbf{P}_{k+1|k} = \mathbf{F}\mathbf{P}_{k|k}\mathbf{F}^T + \mathbf{Q}_k = \mathbf{F}\mathbf{P}_{k|k}\mathbf{F}^T + \mathbf{G}_k\mathbf{G}_k\sigma_v^2 \tag{3b}$$

where $\hat{\mathbf{x}}_{k|k} = E\{\mathbf{x}_k \mid Z^k\}$ is the state estimate at time k with measurements up to k denoted by $Z^k = \{\mathbf{z}_0, \mathbf{z}_1, \ldots, \mathbf{z}_k\}$, $\mathbf{P}_{k|k} = E\{(\mathbf{x}_k - \hat{\mathbf{x}}_{k|k})(\mathbf{x}_k - \hat{\mathbf{x}}_{k|k})^T \mid Z^k\}$ is the estimation error covariance, $\hat{\mathbf{x}}_{k+1|k} = E\{\mathbf{x}_{k+1} \mid Z^k\}$ is the one-step ahead state prediction, and $\mathbf{P}_{k+1|k} = E\{(\mathbf{x}_{k+1} - \hat{\mathbf{x}}_{k+1|k})(\mathbf{x}_{k+1} - \hat{\mathbf{x}}_{k+1|k})^T \mid Z^k\}$ is the prediction error covariance, and the measurement update step:

$$\hat{\mathbf{x}}_{k|k} = \hat{\mathbf{x}}_{k|k-1} + \mathbf{K}_k(\mathbf{z}_k - \mathbf{H}_k\hat{\mathbf{x}}_{k|k-1}) \tag{3c}$$

$$\mathbf{P}_{k|k} = (\mathbf{I} - \mathbf{K}_k\mathbf{H}_k)\mathbf{P}_{k|k-1} \tag{3d}$$

where the Kalman filter gain is given by:

$$\mathbf{K}_k = \mathbf{P}_{k|k-1}\mathbf{H}_k^T\mathbf{S}_k^{-1} \tag{3e}$$

with the measurement prediction error covariance:

$$\mathbf{S}_k = \mathbf{H}_k\mathbf{P}_{k|k-1}\mathbf{H}_k^T + \mathbf{R}_k \tag{3f}$$

In the steady state, the above Kalman filter for the motion and measurement models (1) and (2) becomes the so-called α-β filter with the constant gain denoted by:

$$\mathbf{K}_k = \begin{bmatrix} \alpha & \frac{\beta}{T} \end{bmatrix}^T \tag{4a}$$

where the gains are given by [2, 3, 10, 16]:

$$\alpha = -0.125(\eta^2 + 8\eta - (\eta+4)\sqrt{\eta^2 + 8\mu}) \tag{4b}$$

$$\beta = 2(2-\alpha) - 4\sqrt{1-\alpha} \tag{4c}$$

using the tracking index (target maneuverability index):

$$\eta = T^2\frac{\sigma_v}{\sigma_w} \tag{4d}$$

which can also be viewed as signal to noise ratio (SNR), i.e., the position error caused by constant acceleration $T^2\sigma_v$ vs. the position measurement error σ_w. In the steady state, the transfer function from measurement $\mathbf{z}_k$ to state estimate $\hat{\mathbf{x}}_{k|k}$ is also the Wiener optimal filter.

2.3 Analytic Performance & Design Analysis

A Kalman filter in the steady-state (i.e., the α-β filter) can be viewed as a linear system and so is the truth model. Together, they are driven by random measurement noise, random acceleration input, and deterministic acceleration (maneuver) with unknown in time and magnitude. When $\mathbf{u}_k = 0$ and $\mathbf{v}_k = 0$, the state estimation error covariance position and velocity components contributed to by the sensor noise only (*SNO*) are given by:

$$P_x^{sno} = \frac{2\beta - 3\alpha\beta + 2\alpha^2}{\alpha(4-2\alpha-\beta)}\sigma_w^2 \tag{5a}$$

$$P_{x\dot{x}}^{sno} = \frac{\beta(2\alpha-\beta)}{\alpha(4-2\alpha-\beta)T}\sigma_w^2 \tag{5b}$$

$$P_{\dot{x}}^{sno} = \frac{2\beta^2}{\alpha(4-2\alpha-\beta)T^2}\sigma_w^2 \tag{5c}$$

which show the reduction of variances of the filtered state as compared to the variances of noisy measurements. Similarly, the state estimation error covariance position and velocity components contributed to by a constant acceleration of level A, when $\mathbf{u}_k = A$ and $\mathbf{v}_k = 0$, are given by:

$$P_x^A = \left[(1-\alpha)\frac{T^2}{\beta}A\right]^2 \tag{6a}$$

$$P_{\dot{x}}^A = \left[(\frac{\alpha}{\beta} - 0.5)TA\right] \tag{6b}$$

which are also called the acceleration-induced bias or lag in position and velocity, respectively.

The random process noise is typically used to account for modeling error and uncertainty about target maneuver. When the system is subject to a random acceleration with zero-mean and variance σ_w^2, the state estimation error covariance position and velocity components contributed to by this random acceleration noise (*RAN*), when $\mathbf{u}_k = 0$, are given by:

$$P_x^{ran} = \alpha\sigma_w^2 \tag{7a}$$

$$P_{x\dot{x}}^{ran} = \frac{\beta}{T}\sigma_w^2 \tag{7b}$$

$$P_{\dot{x}}^{ran} = \frac{\beta(\alpha - 0.5\beta)}{T^2(1-\alpha)}\sigma_w^2 \tag{7c}$$

which are the solution of the algebraic Riccati equation (3b) and (3d).

The gains α and β can be related to the damping ratio ζ and bandwidth (undamped natural frequency) ω_n for a continuous-time filter [10, 24] by:

$$\alpha = 2\zeta\sqrt{\beta} - \beta/2 \tag{8a}$$

$$\beta = (\omega_n T)^2 \tag{8b}$$

$$0 < \alpha < 1, \quad 0 < \beta < 2(1-\alpha) \tag{8c}$$

The last condition (8c) ensures the filter stability.

Combining (5) and (6) gives the maximum RMS errors in position and velocity errors:

$$RMS_x^{\max} = \sqrt{P_x^{sno} + P_x^{A_{\max}}} \tag{9a}$$

$$RMS_{\dot{x}}^{\max} = \sqrt{P_{\dot{x}}^{sno} + P_{\dot{x}}^{A_{\max}}} \tag{9b}$$

where A_{max} is the maximum possible acceleration level.

2.4 Illustrative Examples

A target is stationary at x_t = 0 from t = 0 to 200 sec. It then accelerates at u_t = 5 m/s^2 from t = 200 to 400 sec and next moves at the achieved velocity of 1000 m/s from t = 400 to 600 sec. It then decelerates at u_t = -5 m/s^2 from t = 600 to 800 sec and finally stops at x_t = 400 km up to t = 1000 sec. The sampling interval is T = 1 sec. In addition to the deterministic input u_t, a random acceleration $v_t \sim \mathcal{N}(0, 0.1^2)$ (i.e., σ_v = 0.1 m/s^2) is also used in some of the simulation examples presented below.

The target is observed in position by a sensor with its measurement noise standard deviation being σ_w = 5 m. The initial estimation error covariance is $\mathbf{P}_0 = diag([100^2, 10^2])$. The filter is initialized with a sample drawn from $\mathcal{N}\{\mathbf{0}, \mathbf{P}_0\}$.

Fig. 1 shows the Kalman filter gain as a function of time vs. α and β calculated by (4). The position gain is slightly slower than the velocity gain but both converge to the steady state α and β within 50 seconds. For the particular design, the damping ratio is ζ = 0.6398 and the natural frequency is ω_n = 0.1345 rad/sec or 0.0214 Hz, which corresponds roughly to a time constant of 47 sec for transient.

Figs. 2 and 4 compare the RMS errors in position and velocity calculated from 50 Monte Carlo runs (blue), the filter provided error covariance (7) (green), and the predicted maximum errors (9) (red), respectively. The simulated RMS values (blue) match well with the filter predictions (green) in quiescent modes without maneuver, which are zoomed in Figs. 3 and 5. During maneuver, however, the filter predictions (green) remain flat (i.e., erroneous or inconsistent with the reality). In contrast, the maximum errors predicted from (9) (red) with $A_{max} = u_t = \pm 5$ m/s^2 match well with the RMS errors (blue) over the maneuver periods.

Figs. 6 and 7 show position and velocity errors, respectively, where a single run (red) is superimposed with the average (blue). Typical transient behavior for a 2nd order system is visible. The rising time is about 45 sec, consistent with the system bandwidth.

Fig. 8 shows the innovation sequence, a single run (red) and the average (blue), with the predicted measurement error 2σ bounds. The blow-up is shown in Fig. 9 where the upper and lower bounds are in dashed green and red-colored, respectively.

When v_t = 0, the target is driven by the deterministic u_t. The sensor noise only error predictions (5) are shown in Figs. 10 and 11 for position and velocity, respectively. The sensor noise only error predictions (5) (dotted green) match well with the simulated RMS values (aqua) whereas the filter provided error covariance (7) (green) does not, which is *pessimistic* (higher than the actual). Fig. 12 shows the innovation sequence, which is well within its predicted 2σ bounds in quiescent modes but in maneuver periods.

In the above simulation, the analytic formulas match well the numerical results, indicating their usefulness for performance prediction. However, when the actual value of σ_v, σ_w, and A_{max} differs from the one assumed in the filter, the actual tracking errors will be different from those given by the formulas.

This is shown in Figs. 13 through 15 for the position error, velocity error, and innovation, respectively, where the filter uses $(\sigma_w)_{\text{model}} = 2\times(\sigma_w)_{\text{actual}}$. As shown, the predicted values and bounds are larger than the actual ones. The filter is pessimistic or *conservative*. The opposite is also true when the filter uses values smaller than the actual (optimistic). In other words, the prediction will fail when there is a mismatch in model parameters. Hence, it is necessary for a filter to verify its design parameters in run time so as to ensure the operational optimality.

3 Online Monitoring of Optimality

The performance of a tracking filter is expressed in terms of various metrics. There metrics are evaluated over an observation interval, characterizing how far away the state estimate is from the true state in one way or another. Most of these metrics need to know the true state for their calculation. Such metrics are good for design simulation and test experiments where the true state is available.

In this paper, we are interested in those metrics that can be implemented by a tracking filter without knowing the ground truth [19]. One approach is to explore the filter optimality. A well-designed (tuned) Kalman filter should provide an optimal estimate of the state (i.e., minimal error variance). A necessary and sufficient condition for a Kalman filter to be optimal is that its innovation sequence is zero-mean and white.

As a result, these properties should be checked routinely to ensure that the filter is operating properly [7]. If so, the estimation error covariance can be trusted. If not, further tests are needed to determine what may go wrong (diagnosis) and on-line re-tuning may be necessary.

3.1 Tests for Zero-Mean of Innovation Sequence

We first consider a *parametric test*. When the innovation sequence is ergodic and Gaussian, the sample mean can be used to estimate the population mean as test statistic. Consider an individual component of the innovation denoted by $e(k) = z(k) - z(k|k\text{-}1)$.

Denote the true mean and covariance of the innovation by m and R. And denote the sample mean by $\hat{m}$, which is estimated by:

$$\hat{m}(k) = \frac{1}{N}\sum_{t=k}^{k+N-1} e(t) \sim \mathcal{N}\{m, \frac{R}{N}\} \tag{10}$$

where N is the number of samples. Two hypotheses can be formulated as:

$$\begin{aligned} H_0 &\quad m = 0 \\ H_1 &\quad m \neq 0 \end{aligned} \tag{11}$$

The probability of rejecting the null hypothesis H_0 at the α significant level with threshold τ is given by:

$$\mathcal{P}\{\left|\frac{\hat{m}-m}{\sqrt{R/N}}\right| > \frac{\tau - m}{\sqrt{R/N}}\} = \alpha \tag{12}$$

The zero-mean test on each component of the innovation is formulated as:

$$\hat{m} \quad \begin{cases} > \tau & \text{Reject} \quad H_0 \\ < \tau & \text{Accept} \quad H_1 \end{cases} \tag{13}$$

At 5% significant level (α = 0.05), we have:

$$\tau = 1.96\sqrt{\frac{\hat{R}}{N}} \tag{14}$$

where the sample variance is estimated under the null hypothesis as:

$$\hat{R}(k) = \frac{1}{N}\sum_{t=k}^{k+N-1} e^2(t) \tag{15}$$

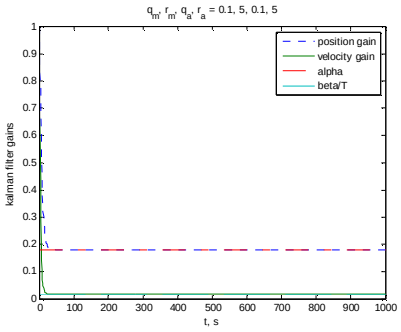

Fig. 1 Kalman vs. α–β Filter Gains

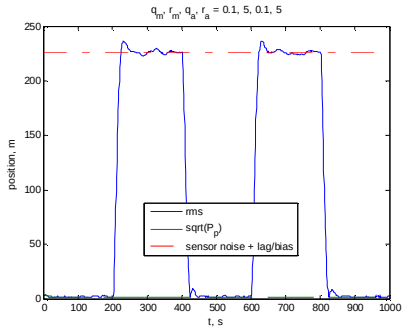

Fig. 2 Monte Carlo Position Errors

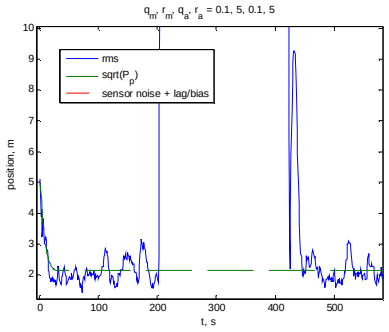

Fig. 3 Position Errors (Blowup of Fig. 2)

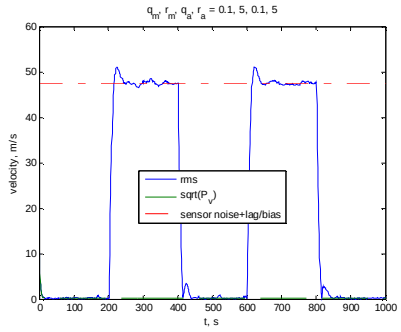

Fig. 4 Monte Carlo Velocity Errors

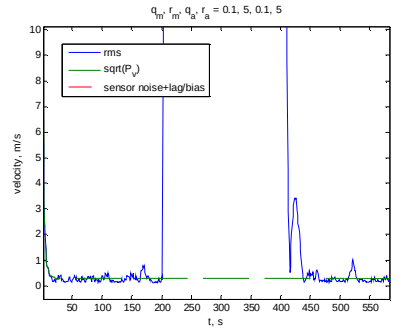

Fig. 5 Velocity Errors (Blowup of Fig. 4)

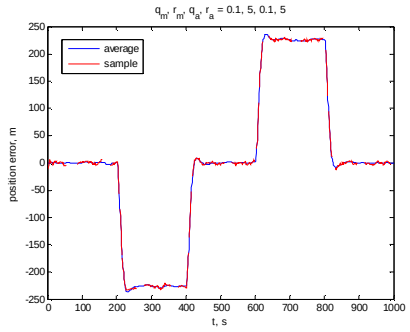

Fig. 6 Sample Behavior of Position Errors

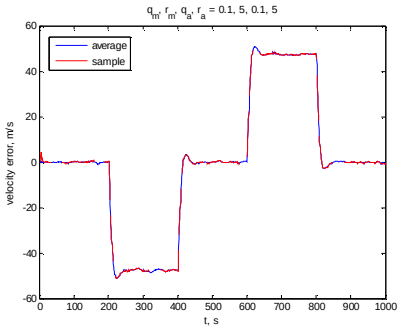

Fig. 7 Sample Behavior of Velocity Errors

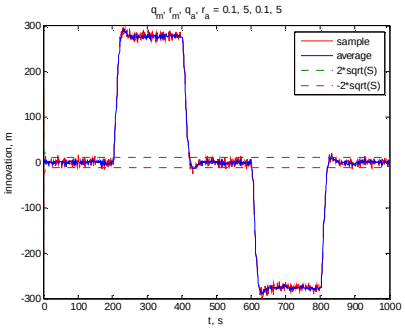

Fig. 8 Sample Behavior of Innovation

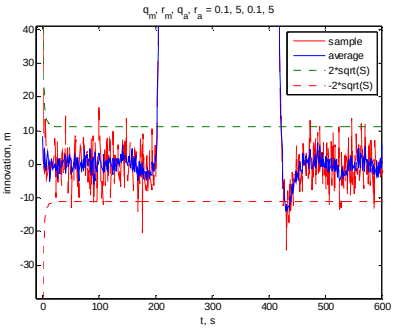

Fig. 9 Blowup of Fig. 8

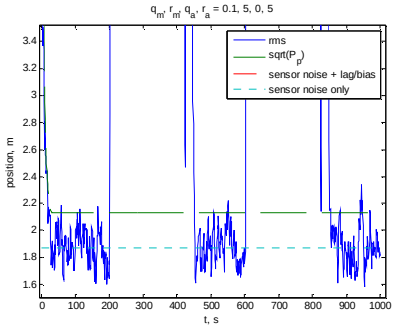

Fig. 10 Position Errors with Sensor Noise Only

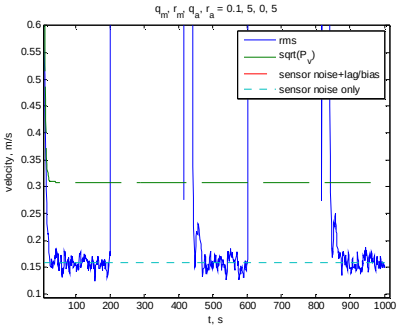

Fig. 11 Velocity Errors with Sensor Noise Only

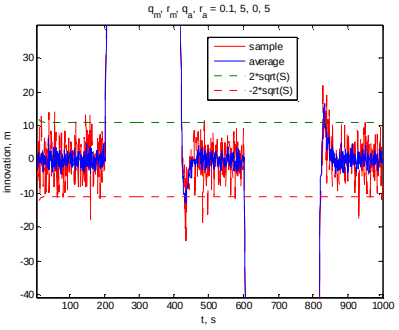

Fig. 12 Innovation with Sensor Noise Only

For *nonparametric test*, an asymptotic relative efficiency (ARE) [11] efficacious small-sample (≈ 10) robust (insensitive to outliers) nonparametric distribution-free linear rank test from the Chernoff-Savage class [8] for testing shift in location is the Mann-Whitney-Wilcoxon (MWW) two-sample statistics [11, 14]. Two independent random batch samples n and m are taken consecutively of the innovations sequence, representing populations X and Y, respectively, where the total number of samples $N = m + n$, the distribution model is $F_Y(x) = F_X(x - \theta)$, and the null hypothesis of identical distributions $H_0 : \theta = 0$. A symmetric version of the MWW [14] test is given by:

$$W = \frac{1}{nm}\sum_{i=1}^{m}\sum_{j=1}^{n}\operatorname{sgn}(x_i - y_j) \tag{16}$$

For selected small sample sizes, the cumulative density function (*cdf*) of W is tabulated. Thus a given value can be stored and compared with a threshold at given level of significance to accept or reject the null hypothesis. While the test requires ranking of

the batched samples, for small sample sizes ($m + n < 20$) the computation time and delay incurred are very small.

3.2 Measurement Screening and Dynamics Detection

In order to both flag and eliminate measurement outliers Tukey's method of Hinges [22] can be used to interpolate quartiles. Given a small, moving batch of ranked data samples, the median of the sample is computed. The data are divided into high and low groups, and the middle (median) values of the groups are denoted as Q1 and Q3, the first and third quartile, respectively. The inter-quartile range (IQR) is computed, i.e., IQR = Q3 – Q1. Next two "fences" are computed as $\text{Fence}_{(\text{lower})}$ = Q1 – 1.5×IQR and $\text{Fence}_{(\text{upper})}$ = Q3 + 1.5×IQR. Values outside the fences are considered outliers. To note, this test was used with great success in eliminating sensor caused outliers with real-time data [15].

The same method can be applied to the innovations sequence. In this case, values outside the fences can be used to detect dynamic changes not accounted for in the filter model.

3.3 Tests for Whiteness of Innovation Sequence

The *parametric* whiteness test is performed to check statistically that the innovation sequence is a white sequence. The sample covariance as a function of delays or lags is used as the test statistic. For a component of the innovation sequence, the sample covariance function is given by:

$$\hat{R}(k,\Delta) = \frac{1}{N}\sum_{t=k}^{k+N-1}[e(t)-\hat{m}(k)][e(t+\Delta)-\hat{m}(k)] \tag{17}$$

where $\Delta = 0, 1, \ldots$, is the delay or lag of the covariance function. The normalized covariance test statistic is defined as:

$$\hat{\rho}(k,\Delta) = \frac{\hat{R}(k,\Delta)}{\hat{R}(k,0)} = \frac{\hat{R}(k,\Delta)}{\hat{R}(k)} \sim \mathcal{N}\{0,\frac{1}{N}\} \tag{18}$$

For $N > 30$, the 95% confidence interval is $\pm 1.96/\sqrt{N}$. For $\Delta = 0$, $\rho(k, \Delta) = 1$ so the interval is $1 \pm 1.96/\sqrt{N}$. For $\Delta \neq 0$, $\rho(k, \Delta) = 0$ so the interval is $\pm 1.96/\sqrt{N}$. Similar tests can be constructed for the cross-covariance properties between innovation components as well.

A more efficient implementation of (16) is to use the fast Fourier transform (FFT) to compute the covariance. Furthermore, the autocorrelation function, $R(\tau)$, of the batch sequence can be used to compute the related power spectral density, $S(f)$, in order to gain an insight into the uniformity (or lack) of the shapes of $S(f)$.

A highly sensitive small sample *nonparametric* test for whiteness is the Shapiro-Wilk [8, 26] test with the null hypothesis that a sample $x_1, \ldots, x_n$ came from a normally distributed population. The test statistic is:

$$W = \frac{(\sum_{i=1}^{n} a_i x_{(i)})^2}{\sum_{i=1}^{n}(x_i - \bar{x})^3} \tag{19}$$

where $x_{(i)}$ (with parentheses enclosing the subscript index i) is the ith order statistic, i.e., the ith-smallest number in the sample, $\bar{x}$ is the sample mean, the constants a_i are given by:

$$[a_1 \quad \cdots \quad a_n] = \frac{\mathbf{m}^T\mathbf{V}^{-1}}{(\mathbf{m}^T\mathbf{V}^{-1}\mathbf{V}^{-1}\mathbf{m}^T)^{1/2}} \tag{20}$$

where $\mathbf{m} = [m_1, \ldots, m_n]^T$ with its elements being the expected values of the order statistics of independent and identically-distributed random variables sampled from the standard normal distribution, and $\mathbf{V}$ is the covariance matrix of those order statistics. The user may reject the null hypothesis if W is too small.

3.4 Tests for Zero-Mean White Gaussian Condition

A simple statistic that contains all the innovation information over some finite window of length N is the weighted sum squared residual (WSSR) [7] defined as:

$$\rho(k) = \sum_{t=k\_N+1}^{k}\mathbf{e}(t)\mathbf{S}^{-1}(t)\mathbf{e}(t) \sim \chi^2\{Np\} \sim \mathcal{N}\{Np, 2Np\} \tag{21}$$

where p is the dimension of $\mathbf{e}(k)$ and $\mathbf{S}(k)$ is obtained from the Kalman filter.

Under the Gaussian assumption for $Np > 30$, the threshold for a level of significance of $\alpha = 0.05$ to accept the null hypothesis is:

$$\tau = Np + 1.96\sqrt{2Np} \tag{22}$$

3.5 Skewness & Kurtosis

When a Kalman filter operates correctly, the innovation sequence is white Gaussian of zero mean. The skewness and kurtosis can be used to characterize the deviation of the data sequence from the normality.

Consider a random variable z. Its skewness and kurtosis are defined respectively as:

$$\gamma_3^z = \frac{E\{(z-m_z)^3\}}{E\{(z-m_z)^2\}^{3/2}} \tag{23}$$

$$\gamma_4^z = \frac{E\{(z-m_z)^4\}}{E\{(z-m_z)^2\}^2} - 3 \tag{24}$$

where $m_z = \mathrm{E}\{z\}$ is the mean value of z. The denominator in (23) and (24) is the variance of z raised in power.

The *skewness* characterizes the degree of asymmetry of a distribution around its mean value. A positive value of skewness corresponds to a distribution with an asymmetric tail extending on the right of the mean whereas a negative value indicates an asymmetric tail to the left. The *kurtosis* measures the relative peakednes or flatness of a distribution.

For a Gaussian variable, both skewness and kurtosis are identically zero. So they offer a measure of the deviation from Gaussianity.

3.6 Sequential Estimation of Noise Characteristics

First and second-order moments of the noise processes can be estimated based on the state estimates produced by the Kalman filter, which provides a means to check on the filter modeling and its proper operation.

Construct N_x samples of most recent state estimate errors:

$$\mathbf{f}_k = \hat{\mathbf{x}}_{k|k} - \hat{\mathbf{x}}_{k|k-1} = \hat{\mathbf{x}}_{k|k} - \mathbf{F}_{k-1}\hat{\mathbf{x}}_{k-1|k-1} \tag{25}$$

If the system has an unknown constant forcing function, it can be estimated as

$$\mathbf{G}_{k-1}\hat{\mathbf{u}}_{k-1} = \frac{1}{N_x}\sum_{j=1}^{N_x}\mathbf{f}_{k-j} \tag{26}$$

Similarly, a bias in the measurement can be estimated based on N_z most recent measurement prediction errors:

$$\hat{\mathbf{r}}_k = \frac{1}{N_z}\sum_{j=1}^{N_z}[\mathbf{z}_{k-j+1} - \mathbf{H}_{k-j+1}(\mathbf{F}_{k-j}\hat{\mathbf{x}}_{k-j} + \mathbf{G}_{k-j}\hat{\mathbf{u}}_{k-j})] \tag{27}$$

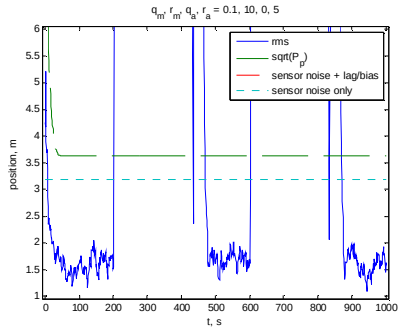

Fig. 13 Position Errors with Parameter Mismatch

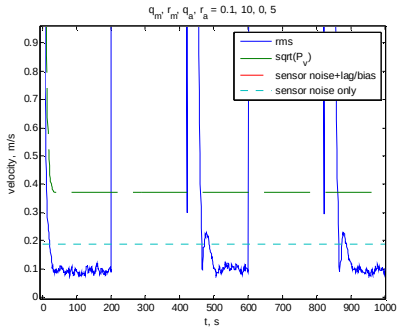

Fig. 14 Velocity Errors with Parameter Mismatch

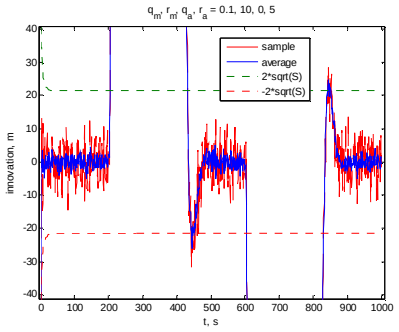

Fig. 15 Innovation with Parameter Mismatch

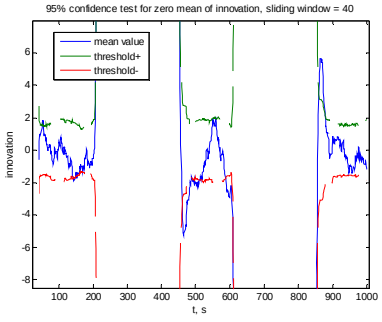

Fig. 16 Zero Mean Test

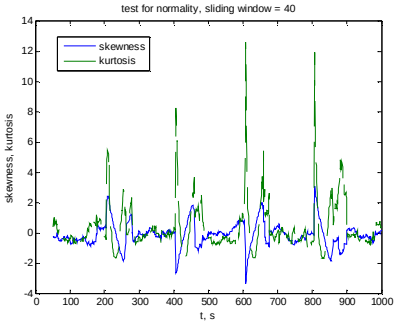

Fig. 17 Skewness & Kurtosis

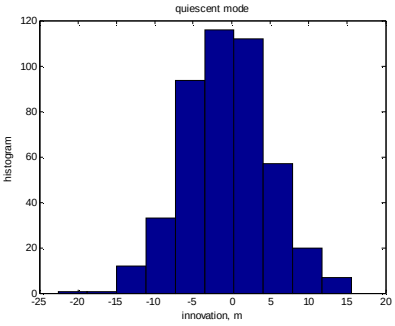

Fig. 18 Histogram of Innovation

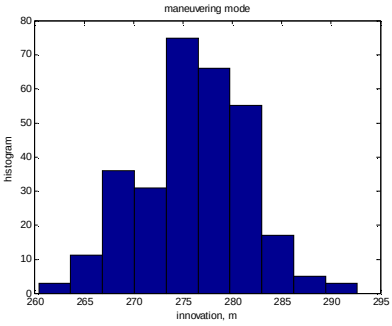

Fig. 19 Histogram of Innovation in Maneuver

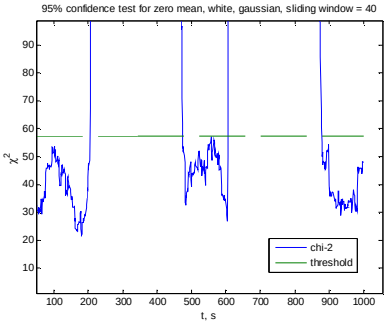

Fig. 20 Zero Mean White Gaussian Test χ^2

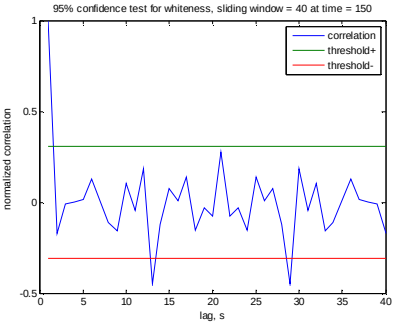

Fig. 21 Normalized Correlation Function

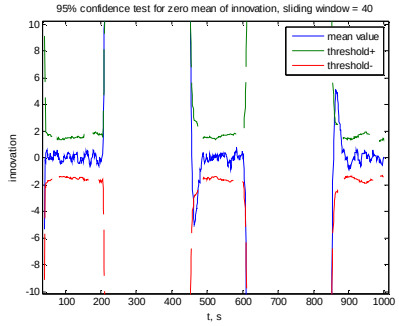

Fig. 22 Zero Mean Test (Sensor Noise Only)

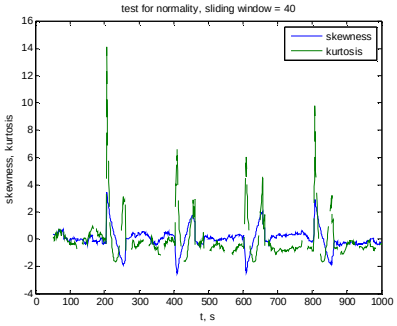

Fig. 23 Skewness & Kurtosis, Sensor Noise Only

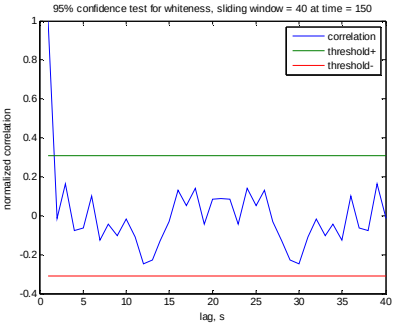

Fig. 24 Correlation (Sensor Noise Only)

It was shown that the bias estimators (26) and (27) are unbiased for optimal state estimates [23]. It was also shown that the following process noise covariance estimator is unbiased [12]:

$$\hat{\mathbf{Q}}_k = \frac{1}{N_x - 1}\sum_{j=1}^{N_x}[(\mathbf{f}'_{k-j+1} - \mathbf{G}_k\hat{\mathbf{u}}'_k)(\mathbf{f}'_{k-j+1} - \mathbf{G}_k\hat{\mathbf{u}}'_k)^T] - \frac{1}{N_x}\sum_{j=1}^{N_x}(\mathbf{F}_{k-j}\mathbf{P}_{k-j}\mathbf{F}_{k-j}^T - \mathbf{P}_{k-j+1}) \quad (28)$$

where

$$\mathbf{f}'_k = \hat{\mathbf{x}}_k - \mathbf{F}_{k-1}\hat{\mathbf{x}}_{k-1} - \mathbf{G}_{k-1}\hat{\mathbf{u}}_{k-1} \quad (29a)$$

$$\mathbf{G}_{k-1}\hat{\mathbf{u}}'_{k-1} = \frac{1}{N_x}\sum_{j=1}^{N_x}\mathbf{f}'_{k-j+1} \quad (29b)$$

The measurement noise covariance is estimated by:

$$\hat{\mathbf{R}}_k = \frac{1}{N_z - 1}\sum_{j=1}^{N_z}[(\tilde{\mathbf{z}}_{k-j+1} - \hat{\mathbf{r}}_k)(\tilde{\mathbf{z}}_{k-j+1} - \hat{\mathbf{r}}_k)^T - \frac{N_z - 1}{N_z}\mathbf{H}_{k-j+1}(\mathbf{F}_{k-j}\mathbf{P}_{k-j}\mathbf{F}_{k-j}^T + \hat{\mathbf{Q}}_{k-j+1})] \quad (30a)$$

where

$$\tilde{\mathbf{z}}_k = \mathbf{z}_k - \mathbf{H}_k(\mathbf{F}_{k-1}\hat{\mathbf{x}}_{k-1} + \mathbf{G}_{k-1}\hat{\mathbf{u}}_{k-1}) \quad (30b)$$

3.7 Robust Statistics & Stochastic Approximation

In addition to simple tests described above, more robust criteria can be used to estimate variance and correlation coefficients so as to make the results less insensitive to outliers and have smaller bias and variations [21]. Examples include the bi-weight method [22] and the square of the absolute median deviation for robust variance estimation [9, 22] and the rank correlation method for estimating correlation coefficients [9].

Stochastic approximation methods (SA) provide an online framework for robust non-parametric parameter estimation [13], system identification [1], and quantile estimation among others [25]. In particular, the Robbins Monroe SA and the robustized minimum variance least-square method can be used to estimate the quantiles of the innovations sequence. The quantiles can be directly related to the known properties of the Gaussian distribution. In conjunction with skewness and kurtosis, it allows characterizing the deviation of the data sequence from Gaussian.

Computation of quantiles. It can be shown that to estimate quantiles of a distribution, the SA recursion is of the form [14, 17]:

$$x_{p+1} = x_p - \frac{1}{p} A_p S_m(x_p, \lambda_k) \quad (31a)$$

where

$$S_m(x_p, \lambda_k) = \frac{1}{m}\sum_{i=1}^{m} \mathrm{sgn}(x_p - Y_{i+m(p-1)}) + (1 - 2\lambda_k) \quad (31b)$$

where Y is the data sequence, assumed to be i.i.d, A_p is an adaptive gain matrix (based on a nonparametric estimator) and λ_k is the selected quantile to be estimated. Note that k quantiles can be simultaneously estimated by this procedure. Further note that the computation of the adaptive A_p requires batch processing and ranking incurring a small delay. Alternatively, a non-adaptive gain coefficient could be used without ranking. However, while streamlining processing it would not possess the robust properties of the adaptive SA.

On-line density estimation. For recursive density estimation, the SA procedure is modified to estimate parameters of a non-orthogonal basis function (translated Beta density function) approximation of an arbitrary density function [14, 17]. The recursion in this case becomes:

$$x_{p+1} = x_p - \frac{1}{p} A_p (x_p - D^{-1}\phi(w_p)) \quad (32)$$

where $\phi(w)$ is the translated Beta density function, and w are the i.i.d random samples from the distribution, and D is band matrix with $2k+1$ nonzero diagonals given by $d_{ij} = <\phi_{ij}, \phi>$.

This method minimizes the integral square error between the "model" and the actual density to be estimated. A *salient feature* of this method is that it does not require storage or ranking and can be used directly on-line to estimate the "empirical" density function as function of time. The characteristics of the empirical density can be compared with respect to the normal density with deviations computed by methods as described above.

3.8 Illustrative Examples

The same simulation scenarios as in Section 2 are used here to illustrate optimality monitoring where the sliding a window length of 40 sec is used, which is roughly equal to the filter transient interval. Fig. 16 shows the test statistic of the zero mean condition for the innovation with upper and lower significant bands on the same plot. For a sample run, the condition is satisfied over the quiescent periods without maneuver. However, it is violated in all maneuver periods.

Fig. 17 shows the skewness (blue) and kurtosis (green) estimated over each sliding window of innovations. After a transient, both estimates go down to small values. Right after a maneuver (initiation and termination), large values appear, indicating deviation from Gaussian. The signs of skewness are consistent of the directions of acceleration-induced biases. The kurtosis shows large concentration (value peaks) right after the initiation and termination of a maneuver.

For a particular run, Figs. 18 and 19 are the histogram of the innovations in the quiescent and maneuver modes, respectively.

Fig. 20 shows the χ^2 test of the innovation, which satisfies the zero-mean white Gaussian condition in quiescent modes but violates it in maneuver modes.

Fig. 21 shows the covariance function. For this particular data window, except for two small spikes, the covariance values at other lags are within the thresholds, indicating no correlation, thus white practically.

The same simulation was run for the sensor noise only case where the random acceleration noise is set to zero $v_t = 0$ with only deterministic acceleration left. Fig. 22 shows the test statistic of the zero mean condition for innovation with upper and lower significant bands. Fig. 23 shows the skewness and kurtosis estimates. Fig. 24 shows the autocorrelation function with upper and lower significant bands.

The results are "cleaner" than the previous case with process noise and all the conclusions about the tests hold.

Additional results for probability of detection and false alarm rate as well as latency of these and other test statistics will be examined in subsequent papers.

4 Adaptive Fusion & Management

In run time, a tracking filter needs to be prepared to handle possible changes in sensor error characteristics and target maneuvers, both leading to model mismatches and if not dealt with properly, would degrade the overall tracking performance.

The optimality self online monitoring (OSOM) procedure described in Section 3 provides means to verify design assumptions and validate operating conditions. Any deviation from the optimality prompts actions. This may range from individual filter tuning, adaptive sensor fusion, active sensor scheduling and management, to network coordination.

4.1 Individual Filter Tuning

It is obvious that when the actual measurement error covariance **R** is found to differ significantly from the assumed value in the filter, the filter ought to be adjusted to reflect the new reality for better performance.

The design procedure described in Section 2 factors in maximum possible maneuver but in a conservative manner. In contrast, proactive methods include reactive adaptation and multiple model estimation [3]. The former includes single filter adaptation, variable dimension filter, two-stage bias estimation, and input estimation. The latter is exemplified by the Multiple Model Adaptive Estimator (MMAE) [20] and Interacting Multiple Model (IMM) algorithm [5].

4.2 Adaptive Fusion with Optimality Monitoring

These maneuver adaptive filtering methods still experience biases or lags in position and velocity estimates after the initiation and termination of a maneuver, although reduced considerably as compared to non-maneuver filters. Such errors are primarily caused by transient behaviors. If these estimates are used in track fusion, the fused track may be "derailed" if different biases or lags from different sensors are not recognized. Since the optimality conditions no longer hold in the innovation, statistical tests similar to those for individual filters as described in Section 3 may be developed to conduct fuser autonomous integrity monitoring (FAIM) to ensure consistent fusion.

4.3 Sensor Management & Network Coordination

One way to reduce transient errors is to obtain a direct estimate of the target maneuver and to correct the tracking filtering accordingly. In the past, change in target orientation from a sequence of visual images was used to deduce target maneuver [27]. Recently, range-Doppler images of a target from a high range resolution (HRR) radar are used to extract target maneuver information [28]. This involves change of sensor modes and coordination of multiple sensors from the same or different platforms.

As described in this paper, the OSOM procedure is a bottom-up approach from individual filters through fusion centers to network managers, which will play a critical role for quality insurance in network-centric layered sensing.

5 Conclusions

In this paper, we reported our initial study of online monitoring of tracking optimality as means for performance evaluation and adaptation. The steady-state Kalman filter in one coordinate, i.e., the α–β filter, was used as an example for illustration. As shown by simulation, the tracking performance could be well predicted when the models were perfectly known. However, it failed when the filter models did no match reality. Various optimality tests applied to the innovation sequence could detect such conditions.

The target state estimate and the corresponding estimation error covariance should be accompanied by an optimality indicator (consistency or integrity indicator) when it is used for track fusion, sensor management, targeting, and control. Our ongoing research in this direction seeks for fast and reliable indicators and metrics and their incorporation to target tracking, sensor fusion, and resource management algorithms.

References

[1] Y. Bar-Shalom, "Application of Stochastic Approximation to On-Line System Identification," *IEEE T-AC*, October 1970, pp. 606-607.

[2] Y. Bar-Shalom and X.R. Li, *Multitarget-Multisensor Tracking: Principles and Techniques*, YBS Publishing, Storrs, CT, 1995.

[3] S. Blackman and R. Popoli, *Design and Analysis of Modern Tracking Systems*, Artech House, Boston, 1999.

[4] E.P. Blasch, A. Rice, and C. Yang, "Relative Track Metrics to Determine Model Mismatch," *Proc. of the SPIE: Signal and Data Processing of Small Targets*, O.E. Drummond (Ed.), Vol. 6236, June 2006.

[5] H. Blom and Y. Bar-Shalom, "The Interacting Multiple Model Algorithm for Systems with Markovian Switching Coefficients," *IEEE Trans. on Automatic Control*, 33(8), 1988.

[6] W.D. Blair, "Tracking Filter Design," *Proc. of 10th ONR/GTRI Workshop on Target Tracking and Sensor Fusion*, Monterey, CA, May 2007.

[7] J.V. Candy, *Signal Processing: the Model-Based Approach*, McGraw-Hill Book Company, New York, 1986.

[8] M. Chernoff and I.R. Savage, "Asymptotic Normality and Efficiency of Certain Nonparametric Tess Statistics," *Ann. Math. Stat*. (29), 1956.

[9] H.A. David, *Order Statistics*, Wiley, New York, 1981.

[10] A. Farina and F.A. Studer, *Radar Data Processing* (Vol. I & II), Wiley, New York, 1985.

[11] J. Gibbons, *Nonparametric Statistical Inference*, McGraw Hill, 1971.

[12] F.D. Groutage, *Adaptive Robust Sequential Estimation with Application to Tracking a Maneuvering Target*, Ph.D. Dissertation, Univ. of Wyoming, May 1982

[13] I. Kadar and L. Kurz, "Robustized Scalar Form of Gladyshev's Theorem with Applications to Non-Linear Systems," *Proc. of the Fourteenth Princeton Conference on Information Sciences and Systems*, March 26-29, 1980.

[14] I. Kadar and L. Kurz "A Robustized Vector Recursive Stabilizer Algorithm for Image Restoration," *Information and Control* (44), 1980.

[15] I. Kadar, *Personal Communication*, February 2008.

[16] P.R. Kalata, "The Tracking Index: A Generalized Parameter for α–β and α–β–ρ Target Trackers," *IEEE Trans. Aerospace and Electronic Systems*, 20(2), March 1984.

[17] P. Kersten. and L. Kurz, "Robustized Vector Robbins-Monro Algorithm with Applications to M-Interval Detection," *Information Sciences* (11), 1976.

[18] X.R. Li and Z.L. Zhao, "Evaluation of Estimation Algorithms. Part I: Local Performance Measures," *IEEE Trans. Aerospace and Electronic Systems*, November 2004.

[19] X. R. Li, "Toward Development of a Theory of Estimation Performance Evaluation," ," *Proc. of 10th ONR/GTRI Workshop on Target Tracking and Sensor Fusion*, Monterey, CA, May 2007.

[20] P. Mayabeck, *Stochastic Models, Estimation, and Control*, Volume 1, Academic Press, Inc, 1979.

[21] A. Moghaddamjoo and R.L. Kirlin, "Robust Adaptive Kalman Filtering with Unknown Inputs," *IEEE Trans. On Acoustics, Speech, and Signal Processing*, 37(8), Aug. 1989.

[22] F. Mosteller and W. Tukey, *Data Analysis and Regression, Academic Press*, New York, 1979.

[23] K.A. Myers and B.D. Tapley, "Adaptive Sequential Estimation with Unknown Noise Characteristics," *IEEE Trans. Automatic Control*, Aug. 1976.

[24] J.H. Painter, D. Kerstetter, and S. Jowers, "Reconciling Steady-State Kalman and Alpha-Beta Filter Design," *IEEE Trans. Aerospace and Electronic Systems*, 26(6), November 1990.

[25] H.T. Wassan, *Stochastic Approximation*, Cambridge Univ. Press 1969.

[26] Wikipedia, *The Shapio-Wilk Test.*

[27] C. Yang, Y. Bar-Shalom, and C.F. Lin, "Maneuvering Target Tracking with Image-Enhanced Measurements," *Proc. of American Control Conf.*, Boston, MA, June 1991.

[28] C. Yang and E. Blasch, "Estimating Target Range-Doppler Image Slope for Maneuver Indication," *Proc. of SPIE Defense and Security 2008: Signal Processing, Sensor Fusion, and Target Recognition XVII*, March 2008, Orlando, FL.